Int. J. Heat Mass Transfer. Vol. 7, pp. 431–446. Pergamon Press 1964. Printed in Great Britain

ANALYTICAL STUDY OF HEAT TRANSFER TO LIQUID METALS IN CROSS-FLOW THROUGH ROD BUNDLES*

CHIA-JUNG HSU
Brookhaven National Laboratory, Upton, New York

(*Received* 10 *June* 1963 *and in revised form* 10 *October* 1963)

Abstract—Improved theoretical expressions for Nusselt numbers are obtained for cross flow of liquid metals through rod bundles, by applying inviscid flow analysis [4, 5]. The theoretical derivations are based upon the assumption that, for a rod located in the interior of a bundle, the circumferential variations of both the tube-wall temperature and the hydrodynamic potential can be expressed by cosine-type distributions. The former assumption is deduced from the experimental observations of Hoe *et al.* [6], under conditions where the heat flux was apparently close to uniform, and the latter is postulated on the basis of theoretical considerations. With these assumptions, the following expression for the Nusselt number, similar to that of Cess and Grosh [5], becomes

$$Nu_t = 0{\cdot}958\,(\phi_1/D)^{\frac{1}{2}}\,(Pe)^{\frac{1}{2}}_{V_{\max}}\,(V/V_{\max})^{\frac{1}{2}}.$$

The above expression predicts Nusselt numbers which agree well with experimental results previously obtained at the Brookhaven National Laboratory [6, 9].

A theoretical method of determining values of the parameter, ϕ_1/D, the normalized hydrodynamic potential drop, is also presented. The results agree well with those obtained experimentally by Cess and Grosh [5]. An analytical expression for ϕ_1/D is obtained by using mathematical functions originally developed by Howland and McMullen [7]. The theoretical values of ϕ_1/D for flow across two typical tube-bank geometries, i.e. square spacing and triangular equilateral spacing, were obtained with the aid of a high-speed digital computer. The numerical results are presented in tabular form.

NOMENCLATURE

A_{2s+1}, B_{2s}, coefficients as defined by equation (17);
C_v, specific heat at constant volume, Btu/lb degF;
D, diameter of a cylinder, ft;
Nu_D, over-all Nusselt number, $h_D D/k$, dimensionless;
Nu_t, over-all Nusselt number, $h_t D/k$, dimensionless;
P, pitch, ft;
Pe, over-all Peclet number, $\rho C_v V D/k$, dimensionless;
$(Pe)_{V_{\max}}$, over-all Peclet number, $\rho C_v V_{\max} D/k$, dimensionless;
R_0, radius of a cylinder, ft;
T, temperature, °F;
T', temperature excess, $T - T_i$, degF;
T'_m, averaged temperature excess, degF;
T_i, uniform upstream temperature, °F;
V, uniform upstream velocity, ft/s;
V_s, fluid velocity on the surface of a cylinder, ft/s;
$V_{\max}$, shell-side fluid velocity across tube bank and based on minimum flow area, ft/s;
a, co-ordinate distance between the centers of cylinders, ft;
c, $\cot \pi\zeta$ as defined by equation (12c);
erfc x, $1 - \dfrac{2}{\sqrt{\pi}}\displaystyle\int_0^x \exp(-\lambda^2)\,d\lambda$;
f_n, polynomials as defined by equation (12b);
h, average heat-transfer coefficient for a given tube, Btu/h ft² degF;
h_t, over-all heat-transfer coefficient based on a specified surface temperature, Btu/h ft² degF;
i, $\sqrt{-1}$;

* This work was performed under the auspices of the U.S. Atomic Energy Commission.

k, thermal conductivity, Btu/h ft degF;
n, integer;
p, co-ordinate distance between the centers of cylinders in different rows, ft;
q, co-ordinate distance between the rows of cylinders, ft;
q', rate of heat flow per unit length of cylinder perpendicular to the direction of flow, Btu/ft h;
q'', surface heat flux, Btu/ft^2 h;
r, radial distance, ft;
s, integer;
t, time, s;
v_r, v_θ, velocity components in r and θ directions;
w_0, w_s, complex functions as defined by equations (7) and (8);
x, the distance along the diameter of cylinder measured from the forward stagnation point, ft;

Greek symbols
${}^s\alpha_n$, coefficient as defined by equation (10);
β, angle measured from the forward stagnation point on cylinder, rad;
δ, parameter;
ζ, ζ_0, complex number as defined by equation (9);
θ, angle, radian or degree;
θ_1, temperature excess at $\beta = \pi/2$, degF;
θ_0, surface temperature excess as defined by equation (2), degF;
θ_a, temperature as defined by equation (2), °F;
θ_m, average surface temperature excess, degF;
κ, thermal diffusivity, ft^2/h;
λ, diameter-to-pitch ratio, D/P, dimensionless;
μ, viscosity of fluid, lb/h ft;
μ_f, absolute fluid evaluated at average film temperature, lb/h ft;
π, $= 3{\cdot}1416\ldots$;
ρ, density of fluid, lb$_m$/ft^3;
ρ_f, fluid density evaluated at average film temperature, lb$_m$/ft^3;
ρ_1, modulus of the complex number, z, as defined by equation (9);
σ, temperature ratio as defined by equation (3);
Φ, hydrodynamic potential function;
Φ_s, hydrodynamic potential on the surface of a cylinder;
ϕ, unit hydrodynamic potential function, $\Phi/-V$;
ϕ_s, unit hydrodynamic potential on the surface of a cylinder;
ϕ_1, unit hydrodynamic potential at the rear stagnation point on a cylinder;
Ψ, hydrodynamic stream function;
ψ, unit hydrodynamic stream function, $\Psi/-V$;
ω, parameter.

INTRODUCTION

THERE have been very few investigations dealing with the cross flow of liquid metals through staggered rod bundles. To the author's knowledge, there have been but one analytical study and three experimental studies reported in the literature. In the only published theoretical study, Grosh and Cess [4], by assuming inviscid potential flow, derived theoretical expressions for the Nusselt numbers for different surface temperature conditions of a single cylinder placed normally to the direction of flow. These results were then extended to cover the case of flow across a rod located in a bundle [5]. Their theoretical Nusselt numbers fell approximately 10–20 per cent below the experimental values reported by Hoe, Dropkin and Dwyer [6]. The purpose of the present study was to extend the analytical treatment of the case of heat transfer to liquid metals flowing across rod bundles.

In the present paper, a theoretical method of estimating values of ϕ_1/D will be first presented. The extension of the results for a single cylinder to one in a rod bundle requires a knowledge of the hydrodynamic potential drop, ϕ_1/D, between the front and rear stagnation points of the rod. The solution of Laplace's equation satisfying the appropriate boundary conditions is utilized to calculate this quantity. The expression for the hydrodynamic potential drop, ϕ_1/D, is derived by making use of a mathematical function proposed by Howland and McMullen many years ago [7]. Theoretical values of ϕ_1/D have been obtained for two typical tube-bank geometries, i.e. tubes with equilateral triangular spacing and with square spacing. The entire computation was carried out with the aid of an IBM 7090 computer. The calculated results are presented in tabular form. These calculated values of ϕ_1/D have been incorporated in the theoretical expressions for the Nusselt number, and comparisons are made with available experimental results.

Also, in the present paper, the derivation of the Nusselt number, Nu_t, for the case of a cosine surface-temperature distribution is presented. This derivation is based upon the assumption that the circumferential variations of both the tube-wall temperature and the hydrodynamic potential on the surface of a cylinder located in the interior of a bundle can be represented by cosine-type distributions. It will be shown that this new expression predicts Nusselt numbers which agree well with the available experimental results.

PREVIOUS STUDIES

A. *Analytical*

The only analytical study which dealt with the heat transfer of low Prandtl number fluids flowing past a single rod or through rod bundles is believed to be that due to Grosh and Cess [4, 5]. By using the following assumptions:

(a) Constant property, non-dissipative flow.
(b) Steady two-dimensional temperature and velocity fields.
(c) Incompressible, non-viscous and irrotational flow.
(d) Negligible eddy transport of heat compared to molecular conduction.
(e) No contact resistance at the solid–liquid interface.
(f) The hydrodynamic potential distribution on the surface of a cylinder located in a rod bundle is linear with respect to $\bar{x}$, the distance along the diameter of the cylinder measured from the forward stagnation point, i.e.

$$\phi = \phi_1 (\bar{x}/D). \tag{1}$$

(g) Interaction of the thermal boundary layers of the cylinders in a rod bundle is negligible.

They derived several different expressions for Nusselt number by prespecifying the thermal condition on the surface of a rod. By assuming the variation of the surface temperature to be of the form:

$$\theta_0 (\beta) = \theta_m - \theta_a \cos \beta \tag{2}$$

and

$$\sigma = \theta_a/\theta_m \tag{3}$$

they obtained the following Nusselt number, Nu_t, for rod bundles:

$$Nu_t = 0{\cdot}718\,(Pe)^{\frac{1}{2}}\,(\phi_1/D)^{\frac{1}{2}}\left(1 + \frac{\sigma}{3}\right). \tag{4}$$

From the experimental results of Hoe *et al.* [6], they further obtained the following expression for calculating the quantity, σ, in equation (4):

$$\sigma = 0{\cdot}10\,(Pe)^{0{\cdot}233}. \tag{5}$$

To compare equation (4) with the experimental results of Hoe *et al.*, Grosh and Cess recalculated the Nusselt number, Nu_t, based upon the definition of heat-transfer coefficient, h_t, given by the equation:

$$h_t = q'/\pi D\theta_m.$$

The average temperature excess, θ_m, was taken as the arithmetic mean of the nine surface-temperature readings obtained from thermocouples spaced 40° apart on the circumference. The comparison is shown in Fig. 8.

B. *Experimental*

The experimental study of heat transfer to liquid metal flowing across rod bundles was first conducted by Hoe *et al.* [6] at Brookhaven National Laboratory. They measured local and over-all heat-transfer coefficients for flow of mercury under conditions of both wetting and non-wetting. The range of Reynolds number covered was from 15000 to 83000. The effect of the Prandtl number was not investigated. The rods were arranged in an equilateral triangular array, for which D/P was 0·727. For a rod located inside the tube bank, they proposed the following empirical expression for the average shell-side heat-transfer coefficient.

$$\bar{h} = 11{\cdot}6\,(DV_{\max}\,\rho_f/\mu_f)^{0{\cdot}52}.$$

The circumferential variation of both the local heat-transfer coefficient and the tube-wall temperature were also measured. With a Reynolds number range of 15000 to 80000 (corresponding to a Peclet number of 330 to 1760), it was reported that the local heat-transfer coefficient varied smoothly from a maximum value at the forward stagnation point to a minimum value at the rear stagnation point. This finding revealed that within the Reynolds number range covered by the experiment, the eddy transport of heat due to the separation of boundary layer and the turbulent wake is not very significant in comparison to the molecular conduction of heat.

A later experimental study at Brookhaven of the heat transfer characteristics of liquid metals in cross flow through a rod bundle is that due to Rickard, Dwyer and Dropkin [9]. In this, both the local and tube-average coefficients were measured for the flow of mercury normal to a staggered rod bundle. The bundle was composed of sixty ½-in tubes, six wide and ten deep, with equilateral-triangular spacing and a D/P of 0·73. The Reynolds number range was 20000 to 200000. The effect of Prandtl number was found to be the same as that of the Reynolds number. The results were, therefore, correlated in terms of the Peclet number, and the following empirical expression was obtained

$$Nu_t = 4{\cdot}03 + 0{\cdot}228\,(Pe)^{0{\cdot}67}_{V_{\max}}. \quad (6)$$

Recently, Borishanskii *et al.* [1] measured local and average coefficients for flow of liquid sodium across a staggered rod bundle. Despite the different material used, their results agreed quite well with those of Hoe *et al.* and Rickard *et al.* The theoretical expressions for the Nusselt number obtained in this study will be compared with the experimental results of Hoe *et al.* and Rickard *et al.* In either case, theoretical value of ϕ_1/D obtained in this study will be incorporated into the theoretical equations.

PRESENT STUDY

A. *Theoretical derivation of the hydrodynamic potential drop, ϕ_1/D*

To calculate the Nusselt numbers for cross flow of liquid metal through rod bundles, it is necessary to know the value of ϕ_1/D [5]. This term appears in the theoretical expression of Nusselt number for rod bundles, and it represents the difference of the normalized hydrodynamic potential between the forward and rear stagnation points of a rod located in the interior of a rod bundle. An analytical method of obtaining this quantity will be presented in the following.

The calculation of ϕ_1/D requires information concerning the distribution of hydrodynamic potential around a rod located in a rod bundle. The latter information can be obtained by solving Laplace's equation for the specified rod bundle under suitable boundary conditions. Due to geometrical symmetry, it is only necessary to determine the potential field inside the shaded area shown in Fig. 1. The potential distribution around the circumference of a rod can then be determined, and eventually the potential difference between the two stagnation points, *a* and *b*, can be calculated. For flow normal to the bundle, as shown in Fig. 1, the distribution of stream and potential lines can be well approximated by those for flow across double infinite rows of cylinders which are in the same geometrical configuration. For the latter case, Howland and McMullen [7] have proposed a certain periodic function which may be used to obtain the distribution of the stream lines. The following complex analytic functions were defined by Howland and McMullen:

$$-w_0 = \log \sin \pi\zeta + \log \sin \pi(\zeta_0 - \zeta) \quad (7)$$

and

$$w_s = \frac{1}{(s-1)!}\frac{d^s}{d\zeta^s}[(-1)^{s-1} \log \sin \pi\zeta - \log \sin \pi(\zeta_0 - \zeta)] \quad (8)$$

where

$$\zeta = z/a = \rho_1 e^{i\theta}, \quad z = x + iy, \quad \zeta_0 = (p + iq)/a. \quad (9)$$

The distances, *a*, *p* and *q*, are explained in Fig. 2. Both (7) and (8) can be expanded, using the Maclaurin's series expansion.

The expansion of w_s, for instance, results in

$$w_s = \zeta^{-s} + \sum_{n=0}^{\infty} {}^{s}a_n \zeta^n \quad (10)$$

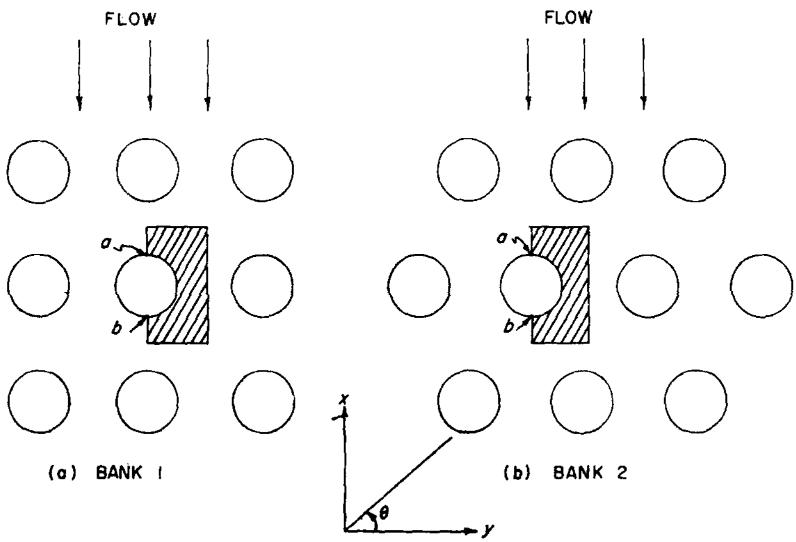

FIG. 1. Schematic representation of flow across tube banks.

with

$$\sigma_n = \sum_{j=1}^{\infty} \frac{1}{j^n} \tag{11}$$

$$f_1(c) = c$$

$$f_n(c) = \left[(1 + c^2)\frac{\mathrm{d}}{\mathrm{d}c}\right]^{n-1} c \tag{12b}$$

$$c = \cot \pi\zeta_0. \tag{12c}$$

The polynomials, f_n, in (12) are

$$f_2(c) = 1 + c^2$$

$$f_3(c) = 2\,c\,(1 + c^2)$$

$$f_4(c) = 2\,(1 + c^2)\,(1 + 3\,c^2)$$

.

.

.

.

$$f_8(c) = 16\,(1 + c^2)\,(315\,c^6 + 525\,c^4 + 231\,c^2 + 17)$$

etc.

Starting with these functions, the stream function for the flow past a double row of cylinders with equal rectangular spacing ($q = a$) was obtained by Howland and McMullen as follows:

$$\begin{aligned}\Psi = &- Vr\cos\theta \\ &+ Va\lambda^2 \{\sum_{n=0}^{\infty} A_{2s+1}[\rho_1^{-(2s+1)}\cos(2n+1)\theta \\ &+ \sum_{n=0}^{\infty} \rho_1^n ({}^s\beta_n \cos n\theta + {}^s\gamma_n \sin n\theta] \\ &+ \sum_{s=1}^{\infty} B_{2s}[\rho_1^{-2s}\sin 2s\theta + \sum_{n=0}^{\infty}\rho_1^n({}^{2s}\delta_n\cos n\theta \\ &+ {}^{2s}\epsilon_n \sin n\theta)]\}\end{aligned} \tag{13}$$

where

$$-1 + A_1 = -^{*}\,\lambda^2\,[\sum_{s=0}^{\infty} {}^{2s+1}\beta_1\,A_{2s+1} - \sum_{s=1}^{\infty} {}^{2s}\gamma_1\,B_{2s}] \tag{14}$$

$$A_{2n+1} = -^{*}\,\lambda^{4n+2}\,[\sum_{s=0}^{\infty} {}^{2s+1}\beta_{2n+1}\,A_{2s+1} - \sum_{s=1}^{\infty} {}^{2s}\gamma_{2n+1}\,B_{2s}] \tag{15}$$

$$B_{2n} = -^{*}\,\lambda^{4n}\,[\sum_{s=0}^{\infty} {}^{2s+1}\gamma_{2n}\,A_{2s+1} + \sum_{s=1}^{\infty} {}^{2s}\beta_{2n}\,B_{2s}] \tag{16}$$

* In the original paper, these (−) signs are missing. Also the numerical values of A's and B's given in the original paper are believed to be in error since they do not seem to satisfy the given boundary condition, i.e $\Psi = 0$, at $\rho_1 = \lambda$.

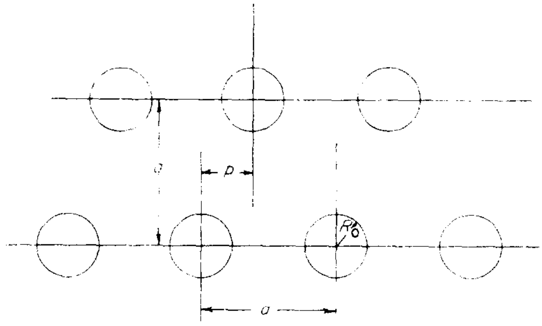

FIG. 2. Co-ordinate system for the potential functions.

and

$$\left.\begin{aligned} A_{2n+1} &= \sum_{r=0}^{\infty} A_{2n+1}^{(r)}, \; A_1^{(0)} = 1, \\ & A_{2n+1}^{(0)} = 0, \; n > 0 \\ B_{2n} &= \sum_{r=0}^{\infty} B_{2n}^{(r)}, \; B_{2n}^{(0)} = 0, \; n > 0 \end{aligned}\right\} \quad (17)$$

$$A_{2n+1}^{(r+1)} = -{}^{*}\,\lambda^{4n+2}\Big[\sum_{s=0}^{\infty} {}^{2s+1}\beta_{2n+1}\, A_{2s+1}^{(r)} - \sum_{s=1}^{\infty} {}^{2s}\gamma_{2n+1}\, B_{2s}^{(r)}\Big] \quad (18)$$

$$B_{2n}^{(r+1)} = -{}^{*}\,\lambda^{4n}\Big[\sum_{s=0}^{\infty} {}^{2s+1}\gamma_{2s}\, A_{2s+1}^{(r)} + \sum_{s=1}^{\infty} {}^{2s}\beta_{2n}\, B_{2s}^{(r)}\Big]. \quad (19)$$

The β and γ coefficients are given in [7].

In the present study, (13) is rearranged into a more convenient form. Noting that $\rho_1 = r/a$, $a = R_0/\lambda$, and then collecting the terms with $\cos\theta$, $\cos(2n+1)\theta$, and $\sin 2n\theta$, (13) can be rearranged to read

$$\begin{aligned} \Psi = & -Vr\cos\theta + VR_0\cos\theta\,\{A_1(R_0/r) \\ & + \lambda^2 (r/R_0)\Big[\sum_{s=0}^{\infty} A_{2s+1}\,{}^{2s+1}\beta_1 + \sum_{s=1}^{\infty} B_{2s}\,{}^{2s}\delta_1\Big]\} \\ & + VR_0\lambda\,\{A_{2n+1}\,\lambda^{-(2n+1)}\,(r/R_0)^{-(2n+1)} \\ & + \lambda^{2n+1}(r/R_0)^{2n+1}\Big[\sum_{s=0}^{\infty} A_{2s+1}\,{}^{2s+1}\beta_{2n+1} \\ & + \sum_{s=1}^{\infty} B_{2s}\,{}^{2s}\delta_{2n+1}\Big]\}\cos(2n+1)\theta \\ & + VR_0\lambda\,\{B_{2n}\,\rho_1^{-2n} + \rho_1^{2n}\Big[\sum_{s=0}^{\infty} A_{2s+1}\,{}^{2s+1}\gamma_{2n} \\ & + \sum_{s=1}^{\infty} B_{2s}\,{}^{2s}\epsilon_{2n}\Big]\}\sin 2n\theta. \end{aligned} \quad (20)$$

* Cf. footnote on page 435

Combining (20) with (14), (15) and (16), and simplifying, yields:

$$\begin{aligned} \Psi = VR_0\Big(&\sum_{n=0}^{\infty}\{A_{2n+1}\,\lambda^{-2n}\,[(R_0/r)^{2n+1} \\ & - (r/R_0)^{2n+1}]\cos(2n+1)\theta\} \\ & + \sum_{n=1}^{\infty}\{B_{2n}\,\lambda^{-2n+1}\,[(R_0/r)^{2n} \\ & - (r/R_0)^{2n}]\sin 2n\theta\}\Big). \end{aligned} \quad (21)$$

(21) is of a form which is amenable to mathematical manipulation. The velocity of fluid on the surface of the cylinder, for instance, can be obtained as follows:

$$\begin{aligned} V_s = & -\left(\frac{\partial\Psi}{\partial r}\right)_{r=R_0} \\ = & -2V\Big\{\sum_{n=0}^{\infty}[A_{2n+1}\,\lambda^{-2n}\,(2n+1) \\ & \cos(2n+1)\theta] + \sum_{n=1}^{\infty}[B_{2n}\,\lambda^{-2n+1}\,(2n)\sin 2n\theta]\Big\}. \end{aligned} \quad (22)$$

From (22), it can be shown that the fluid velocity is zero at the front ($\theta = \pi/2$) and rear stagnation points ($\theta = 3\pi/2$).

The present objective is to determine the potential field. This can be achieved by utilizing the relationship

$$\Phi = -\int r\,\frac{\partial\Psi}{\partial r}\,\mathrm{d}\theta. \quad (23)$$

Ultimately, the potential field is obtained as

$$\begin{aligned} \Phi = VR_0\Big(&\sum_{n=0}^{\infty}\{A_{2n+1}\,\lambda^{-2n}\,[(R_0/r)^{2n+1} \\ & + (r/R_0)^{2n+1}]\sin(2n+1)\theta\} \\ & - \sum_{n=1}^{\infty}\{B_{2n}\,\lambda^{-2n+1}\,[(R_0/r)^{2n} \\ & + (r/R_0)^{2n}]\cos 2n\theta\}\Big). \end{aligned} \quad (24)$$

The distribution of hydrodynamic potential around a rod located in the interior of a rod bundle can be calculated using (24). By letting $r = R_0$, one gets

$$\begin{aligned} \Phi_s = 2VR_0\Big[&\sum_{n=0}^{\infty} A_{2n+1}\,\lambda^{-2n}\sin(2n+1)\theta \\ & - \sum_{n=1}^{\infty} B_{2n}\,\lambda^{-2n+1}\cos 2n\theta\Big]. \end{aligned} \quad (25)$$

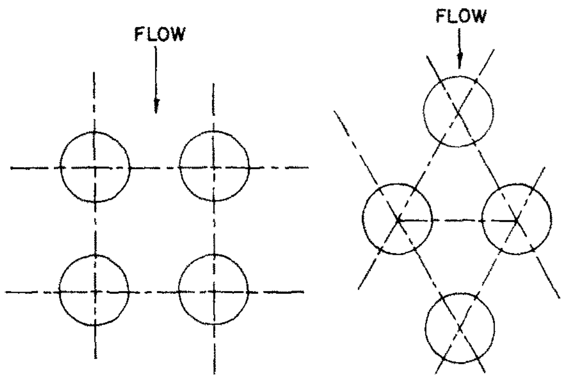

(a) BANK 1
SQUARE SPACING

(b) BANK 2
EQUILATERAL TRIANGULAR SPACING

FIG. 3. Schematic representation of tube bank geometries.

The difference in hydrodynamic potential between the front and rear stagnation points, ϕ_1/D, can be found by calculating the difference of Φ_s at $\theta = \pi/2$ and $\theta = 3\pi/2$. Finally, this is given by the equation

$$\phi_1/D = 2 \sum_{n=0}^{\infty} (-1)^n \lambda^{-2n} A_{2n+1} \qquad (26)$$

where $\lambda = \frac{1}{2}(D/P)$ and the A's are as represented by (17) and (18). It is not difficult to show that the infinite series on the right-hand side of (26) will approach unity when the value of D/P, "diameter-to-pitch" ratio, approaches zero. This corresponds to the case when a single cylinder is placed inside a uniform fluid stream; and, as expected, (26) reduces to $\phi_1/D = 2{\cdot}0$.

For a rod bundle with equilateral triangular spacing, such as that shown in Fig. 3(b), (26) is still valid. For this case, however, the argument, c, must be modified. For this configuration, $p = a/2$, and consequently,

$$c = \cot(i\pi q/a + \pi/2) = -i \tanh(\pi q/a). \qquad (27)$$

The hydrodynamic potential drop, ϕ_1/D, for two typical tube bank geometries, as shown in Fig. 3, was calculated as a function of D/P. The mathematical computation was performed with the aid of an IBM 7090. To assure the convergence of the infinite series, the Maclaurin's series expansion coefficient was evaluated up to the 25th term. The twenty-five b constants [7], b_1 through b_{25}, for both cases are tabulated in Table 1. The convergence of the infinite series was found to be good within the range of D/P used. The calculated values of ϕ_1/D are tabulated in Table 2.

Table 1. Calculated values of b_n in (19)

	Bank 1	Bank 2
b_1	$-3{\cdot}15335$	$-3{\cdot}11452$
b_2	$-0{\cdot}369815 \times 10^{-1}$	$0{\cdot}847310 \times 10^{-1}$
b_3	$0{\cdot}780345 \times 10^{-1}$	$-0{\cdot}174414$
b_4	$0{\cdot}123033$	$-0{\cdot}271576$
b_5	$-0{\cdot}157498$	$0{\cdot}326546$
b_6	$-0{\cdot}169172$	$0{\cdot}320401$
b_7	$0{\cdot}161246$	$-0{\cdot}242412$
b_8	$0{\cdot}140183$	$-0{\cdot}126639$
b_9	$-0{\cdot}118284$	$0{\cdot}169492 \times 10^{-2}$
b_{10}	$-0{\cdot}999332 \times 10^{-1}$	$-0{\cdot}993702 \times 10^{-1}$
b_{11}	$0{\cdot}883536 \times 10^{-1}$	$0{\cdot}156051$
b_{12}	$0{\cdot}806613 \times 10^{-1}$	$0{\cdot}166686$
b_{13}	$-0{\cdot}759076 \times 10^{-1}$	$-0{\cdot}132108$
b_{14}	$-0{\cdot}715676 \times 10^{-1}$	$-0{\cdot}709479 \times 10^{-1}$
b_{15}	$0{\cdot}671093 \times 10^{-1}$	$0{\cdot}994044 \times 10^{-4}$
b_{16}	$0{\cdot}629110 \times 10^{-1}$	$-0{\cdot}622787 \times 10^{-1}$
b_{17}	$-0{\cdot}589763 \times 10^{-1}$	$0{\cdot}101615$
b_{18}	$-0{\cdot}554786 \times 10^{-1}$	$0{\cdot}110877$
b_{19}	$0{\cdot}524518 \times 10^{-1}$	$-0{\cdot}910285 \times 10^{-1}$
b_{20}	$0{\cdot}498253 \times 10^{-1}$	$0{\cdot}500030 \times 10^{-1}$
b_{21}	$-0{\cdot}474955 \times 10^{-1}$	$0{\cdot}135303 \times 10^{-3}$
b_{22}	$-0{\cdot}453773 \times 10^{-1}$	$-0{\cdot}452236 \times 10^{-1}$
b_{23}	$0{\cdot}434224 \times 10^{-1}$	$0{\cdot}750400 \times 10^{-1}$
b_{24}	$0{\cdot}416113 \times 10^{-1}$	$0{\cdot}831057 \times 10^{-1}$
b_{25}	$-0{\cdot}399474 \times 10^{-1}$	$-0{\cdot}691281 - 10^{-1}$

The comparison of the theoretical hydrodynamic potential drop, ϕ_1/D, calculated in this study, with that obtained by Grosh and Cess

Table 2. Theoretical values of the hydrodynamic potential drop, ϕ_1/D

D/P	ϕ_1/D (Bank 1)	ϕ_1/D (Bank 2)	D/P	ϕ_1/D (Bank 1)	ϕ_1/D (Bank 2)
0·00	2·0000	2·0000	0·44	2·3805	2·3381
0·01	2·0002	2·0002	0·45	2·4012	2·3557
0·02	2·0007	2·0006	0·46	2·4227	2·3740
0·03	2·0015	2·0014	0·47	2·4451	2·3929
0·04	2·0027	2·0025	0·48	2·4684	2·4125
0·05	2·0042	2·0039	0·49	2·4927	2·4328
0·06	2·0061	2·0056	0·50	2·5179	2·4539
0·07	2·0083	2·0077	0·51	2·5442	2·4757
0·08	2·0108	2·0100	0·52	2·5715	2·4983
0·09	2·0137	2·0127	0·53	2·6000	2·5218
0·10	2·0169	2·0157	0·54	2·6297	2·5461
0·11	2·0205	2·0190	0·55	2·6606	2·5713
0·12	2·0245	2·0226	0·56	2·6929	2·5976
0·13	2·0288	2·0266	0·57	2·7265	2·6248
0·14	2·0334	2·0309	0·58	2·7617	2·6531
0·15	2·0385	2·0355	0·59	2·7984	2·6826
0·16	2·0439	2·0405	0·60	2·8368	2·7132
0·17	2·0496	2·0458	0·61	2·8769	2·7452
0·18	2·0558	2·0514	0·62	2·9189	2·7785
0·19	2·0623	2·0574	0·63	2·9630	2·8132
0·20	2·0693	2·0637	0·64	3·0091	2·8496
0·21	2·0766	2·0704	0·65	3·0575	2·8876
0·22	2·0844	2·0775	0·66	3·1084	2·9273
0·23	2·0925	2·0849	0·67	3·1619	2·9690
0·24	2·1011	2·0927	0·68	3·2182	3·0129
0·25	2·1101	2·1008	0·69	3·2776	3·0589
0·26	2·1196	2·1094	0·70	3·3402	3·1074
0·27	2·1295	2·1183	0·71	3·4064	3·1587
0·28	2·1398	2·1276	0·72	3·4765	3·2128
0·29	0·1507	2·1374	0·73	3·5508	3·2702
0·30	2·1620	2·1475	0·74	3·6297	3·3311
0·31	2·1738	2·1580	0·75	3·7137	3·3960
0·32	2·1862	2·1690	0·76	3·8032	3·4652
0·33	2·1990	2·1804	0·77	3·8988	3·5393
0·34	2·2124	2·1923	0·78	4·0013	3·6189
0·35	2·2264	2·2046	0·79	4·1113	3·7047
0·36	2·2409	2·2174	0·80	4·2299	3·7975
0·37	2·2561	2·2306	0·81	4·3581	3·8983
0·38	2·2718	2·2444	0·82	4·4971	4·0082
0·39	2·2882	2·2587	0·83	4·6486	4·1288
0·40	2·3052	2·2734	0·84	4·8143	4·2617
0·41	2·3229	2·2888	0·85	4·9967	4·4091
0·42	2·3414	2·3046	0·86	5·1985	4·5737
0·43	2·3605	2·3211			

using analogical methods, is shown in Figs. 4 and 5. From the plots, it is seen that the agreement between the two is almost perfect up to a D/P ratio of approximately 0·2. Beyond this value, the two are still in satisfactory agreement. In the former range of D/P, the tubes are spaced relatively far apart. For the latter, the tubes are spaced more closely, and consequently more experimental error may be expected.

B. *Derivation of the theoretical Nusselt numbers*

The following derivations for the Nusselt number, Nu_t, are based upon the same assumptions used by Grosh and Cess [4, 5]. These

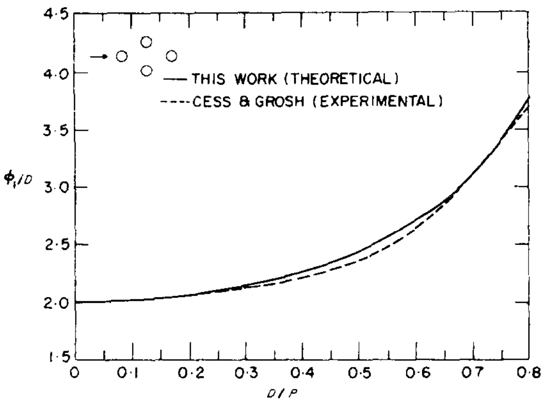

FIG. 4. Comparison of the values of ϕ_1/D obtained by theory and conducting sheet analogy (Bank 2).

assumptions have been listed in the previous section. The assumption of an inviscid flow is equivalent to assuming slug flow around a cylinder. As pointed out by Grosh and Cess, when the Prandtl number becomes extremely small, the heat-transfer rate calculated from viscous flow theory could approach that calculated by non-viscous theory.

Assumption (d) appears, on the basis of experimental evidence, to be reasonably valid. Experimental measurements by both Hoe *et al.* [6] and Borishanskii *et al.* [1], showed that at a Peclet number as high as 1800 ($Re = 83000$), the local heat-transfer coefficient decreased gradually from the forward to the rear stagnation points. In other words, there is no second maximum of the heat-transfer coefficient at about 110° from the forward stagnation point, as there is for non-metallic fluids. This is due to the high thermal conductivity of liquid metals which tends to suppress the effect of eddy transport of heat. For the case of in-line flow of mercury through a rod bundle, Maresca and Dwyer [8] also observed that the eddy transport of heat was not significant until a Reynolds number of approximately 40000 was reached.

Justification of assumption (f) will be presented in the later section of this paper.

With the assumptions, the energy equation in cylindrical co-ordinates can be written as

$$v_r \frac{\partial T}{\partial r} + \frac{v_\theta}{r}\frac{\partial T}{\partial \theta} = \kappa \left[\frac{\partial^2 T}{\partial r^2} + \frac{1}{r}\frac{\partial T}{\partial r} + \frac{1}{r^2}\frac{\partial^2 T}{\partial \theta^2}\right] \tag{28}$$

and, the equation of continuity and the r, θ momentum equations can be replaced by the Laplace equation, i.e.

$$r\frac{\partial^2 \Phi}{\partial r^2} + \frac{\partial \Phi}{\partial r} + \frac{1}{r}\frac{\partial^2 \Phi}{\partial \theta^2} = 0 \tag{29.1}$$

or

$$r\frac{\partial^2 \Psi}{\partial r^2} + \frac{\partial \Psi}{\partial r} + \frac{1}{r}\frac{\partial^2 \Psi}{\partial \theta^2} = 0 \tag{29.2}$$

where

$$v_r = -\frac{1}{r}\frac{\partial \Psi}{\partial \theta} = -\frac{\partial \Phi}{\partial r} \tag{30}$$

and

$$v_\theta = \frac{\partial \Psi}{\partial r} = -\frac{1}{r}\frac{\partial \Phi}{\partial \theta}. \tag{31}$$

If the co-ordinates are transformed from r, θ to ψ and ϕ [2], the mathematical procedure of solving (28) and (29) can be simplified. Thus, after the change of independent variables from r, θ to ψ, ϕ, (28) can be transformed to:

$$V\frac{\partial T}{\partial \phi} = \frac{k}{\rho C_v}\left(\frac{\partial^2 T}{\partial \phi^2} + \frac{\partial^2 T}{\partial \psi^2}\right). \tag{32}$$

Geometrically, this transformation maps the circular cylinder into a flat plate and gives rise to a flow field with constant velocity, V. As shown in Fig. 6, the stream lines (ψ = constant) and the potential lines (ϕ = constant) are mapped into a set of orthogonal straight lines.

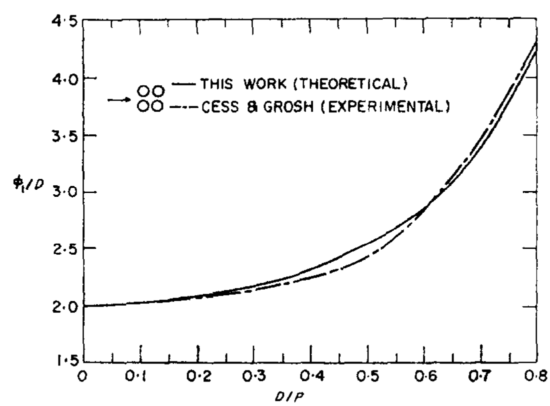

FIG. 5. Comparison of the values of ϕ_1/D obtained by theory and conducting sheet analogy (Bank 1).

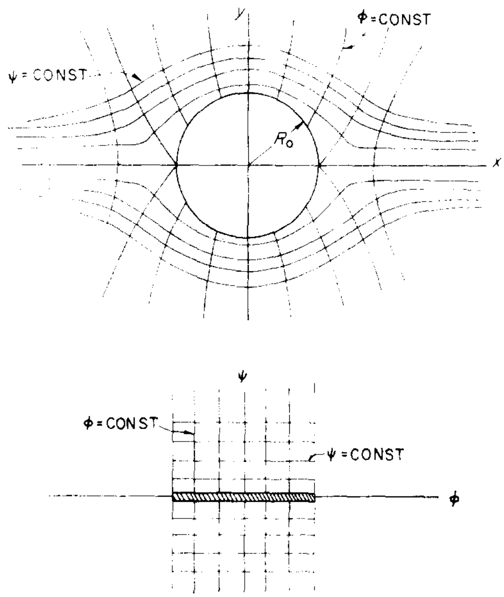

FIG. 6. Co-ordinate system for mapping of a cylinder into a flat plate.

If the term representing the conductive heat transfer in the direction of flow, $\partial^2 T/\partial\phi^2$, is ignored, in comparison to the term representing the convective heat transfer in the same direction, $\partial T/\partial\phi$, (32) can be further simplified to

$$V\frac{\partial T}{\partial \phi} = \frac{k}{\rho C_v}\frac{\partial^2 T}{\partial \psi^2}. \tag{33}$$

(33) is equivalent to the basic differential equation used by Grosh and Cess in their analysis.

(a) *Nusselt number, Nu_t, for cosine surface temperature distribution.* If a change in the temperature variable is made by letting $T' = T - T_i$, (33) then becomes

$$V\frac{\partial T'}{\partial \phi} = \frac{k}{\rho C_v}\frac{\partial^2 T'}{\partial \psi^2}. \tag{34}$$

The dependent variable, T', designates the temperature excess above the approaching uniform stream temperature, T_i.

From Hoe's experimental measurements, it is observed that the circumferential distribution of the surface temperature of a rod located in the interior of rod bundle corresponds fairly closely to a cosine distribution. This is illustrated in Fig. 7, where the excess tube-wall temperature is compared with a cosine curve, for two different surface heat fluxes. It therefore seems plausible to express the tube-wall temperature distribution by the following equation.

$$T' = \theta_1 (1 - \cos\beta) \tag{35}$$

where θ_1 is the temperature excess at $\beta = \pi/2$. From (1), the distribution of hydrodynamic potential on the surface of a cylinder can be written as

$$\phi = \left(\frac{\phi_1}{2D}\right) D (1 - \cos\beta) = \frac{\phi_1}{2}(1 - \cos\beta). \tag{36}$$

Combining (35) and (36) then gives

$$T' = (2\theta_1/\phi_1)\,\phi. \tag{37}$$

It is thus seen that the cosine temperature distribution around the circumference of a rod corresponds to a linear temperature distribution along the surface of a flat plate.

The appropriate boundary conditions for (34) are then

$$\left.\begin{array}{lll} \text{at } \psi = 0,\ 0 < \phi < \phi_1 & T' = (2\theta_1/\phi_1)\,\phi \\ \text{at } \psi = \infty,\ 0 < \phi < \phi_1 & T' = 0 \\ \text{at } \phi = 0,\ \psi > 0 & T' = 0 \end{array}\right\} \tag{38}$$

and the solution of (34), with these boundary conditions, can be obtained by applying Duhamel's theorem to the solution for a constant surface temperature. It is given as [3],

$$T' = 4\,(2\theta_1/\phi_1)\,\phi i^2 \operatorname{erfc}\frac{\psi}{2}\sqrt{[(\rho C_v V)/(k\phi)]}. \tag{39}$$

The local surface heat flux is, therefore,

$$q''(\phi) = -k\,(\partial T'/\partial\psi)_{\psi=0} = \frac{4\theta_1}{\phi_1}\sqrt{[(k\rho C_v V\phi)/\pi]} \tag{40}$$

and, the rate of heat flow over the entire cylindrical surface is given by

$$q' = \frac{8\theta_1}{\phi_1}\sqrt{[(k\rho C_v V)/\pi]}\int_0^{\phi_1}\phi^{1/2}\,d\phi = \frac{16\theta_1}{3}\sqrt{[(k\rho C_v V)/\pi]}\,\phi_1^{1/2}.$$

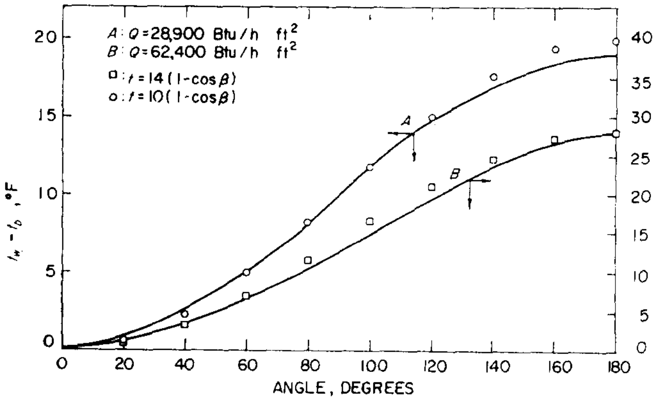

FIG. 7. Comparison of outside tube-wall temperature with cosine curves.

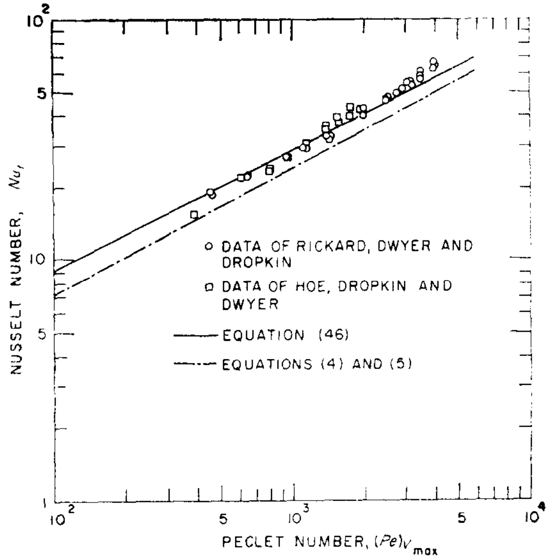

FIG. 8. Comparison of theoretical equations (cosine tube-wall temperature distribution) with experimental results of Hoe *et al.* and Rickard *et al.*

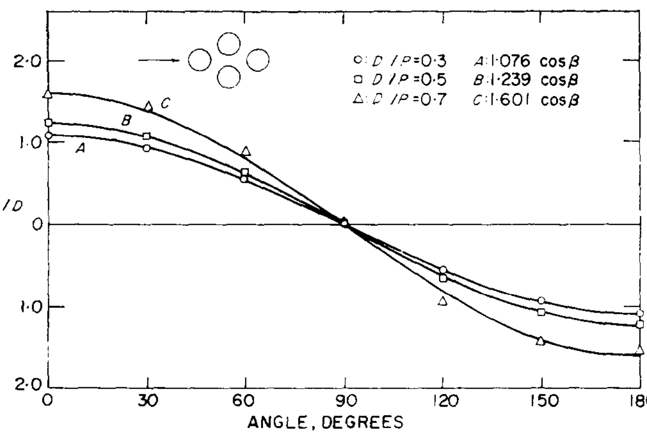

FIG. 9. Comparison of the hydrodynamic potential on the surface of a cylinder with cosine curves (Bank 2).

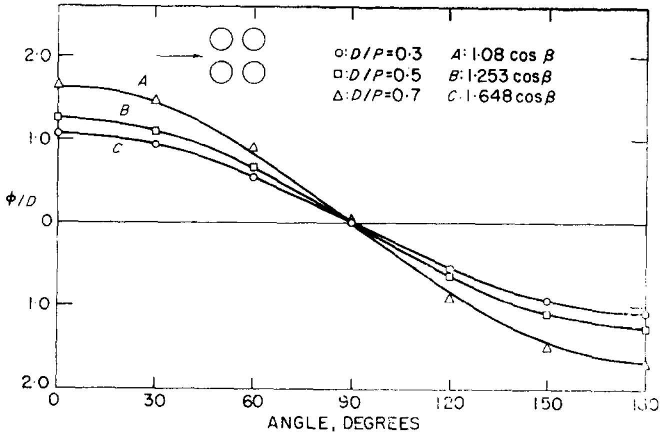

FIG. 10. Comparison of the hydrodynamic potential on the surface of a cylinder with cosine curves (Bank 1).

The average temperature excess over the surface of the cylinder is

$$T'_m = \frac{1}{\phi_1} \int_0^{\phi_1} (2\theta_1/\phi_1)\, \phi \, d\phi = \theta_1. \qquad (41)$$

Therefore, the average heat-transfer coefficient, h_t, is

$$h_t = \frac{q'}{\pi D T'_m} = \frac{16\sqrt{\phi_1}}{3\pi D} \sqrt{[(kC_v\rho V)/\pi]}. \qquad (42)$$

The expression for Nusselt number, Nu_t, is therefore,

$$Nu_t = \frac{h_t D}{k} = \frac{16}{3\pi^{3/2}} \sqrt{(Pe)}\, \sqrt{(\phi_1/D)} \qquad (43)$$

or

$$Nu_t = 0{\cdot}958\, (\phi_1/D)^{1/2}\, (Pe)^{1/2}. \qquad (44)$$

In the above derivation, the Peclet number is based upon the average approaching fluid velocity, V. However, when dealing with flow across rod bundles, the Peclet number is usually based on the average fluid velocity through the minimum free area, $V_{\max}$. These two different expressions for the Peclet number are related by the equation

$$Pe = (Pe)_{V_{\max}}\, (V/V_{\max}). \qquad (45)$$

Consequently, (44) can be written in the alternative form:

$$Nu_t = 0{\cdot}958\, (\phi_1/D)^{1/2}\, (Pe)^{1/2}_{V_{\max}}\, (V/V_{\max})^{1/2}. \qquad (46)$$

In Fig. 8 (46) is compared with the experimental results of Hoe, Dropkin, and Dwyer [6]. As mentioned earlier, the equation obtained by Cess and Grosh, equation (4), is also plotted. The theoretical value of ϕ_1/D used for this case is 3·27. From Fig. 8 it can be seen that the prediction of Nusselt number by means of (44) agrees more closely with results of Hoe *et al.* It should also be pointed out that no empirical correlation such as (5) is necessary in using (44) and (46).

Comparison of (46) with the results of Rickard, Dwyer and Dropkin [9] is also shown in Fig. 8. The results of Rickard *et al.* are those without gas entrainment. The comparison shows that the agreement between (46) and the experimental results is quite good up to a Peclet number of approximately 2000. For the range where the Peclet number exceeds 2000, the experimental results tend to show higher values than the theoretical predictions. This presumably is due to the fact that eddy transport of heat is becoming significant in this range of the Peclet number. For practical situations, however, the Peclet number would seldom exceed 5000. (46) together with the theoretical values of ϕ_1/D given in Table 2 are, therefore, useful in making theoretical predictions.

In deriving (44), it was assumed that the distribution of hydrodynamic potential on the surface of a cylinder located in the interior of a rod bundle could be represented by (36). A similar assumption was made by Grosh and Cess in extending their theory for flow past a single cylinder to that through a rod bundle.

Table 3. Calculated values of A_{2n+1} in (24)

	$D/P = 0{\cdot}30$ Bank 1	$D/P = 0{\cdot}30$ Bank 2	$D/P = 0{\cdot}50$ Bank 1	$D/P = 0{\cdot}50$ Bank 2	$D/P = 0{\cdot}70$ Bank 1	$D/P = 0{\cdot}70$ Bank 2
A_1	1·0819	1·0755	1·2664	1·2428	1·7065	1·6350
A_3	$2{\cdot}0623 \times 10^{-5}$	$3{\cdot}9848 \times 10^{-5}$	$5{\cdot}2195 \times 10^{-4}$	$9{\cdot}9088 \times 10^{-4}$	$5{\cdot}6119 \times 10^{-3}$	$9{\cdot}9673 \times 10^{-3}$
A_5	$1{\cdot}9023 \times 10^{-8}$	$6{\cdot}9419 \times 10^{-10}$	$3{\cdot}6857 \times 10^{-6}$	$1{\cdot}6907 \times 10^{-7}$	$1{\cdot}4654 \times 10^{-4}$	$1{\cdot}9673 \times 10^{-5}$
A_7	$2{\cdot}8102 \times 10^{-12}$	$9{\cdot}4984 \times 10^{-12}$	$4{\cdot}4401 \times 10^{-9}$	$1{\cdot}4363 \times 10^{-8}$	$9{\cdot}3362 \times 10^{-7}$	$2{\cdot}4403 \times 10^{-6}$
A_9	$4{\cdot}7987 \times 10^{-15}$	$4{\cdot}7691 \times 10^{-15}$	$5{\cdot}5648 \times 10^{-11}$	$5{\cdot}4977 \times 10^{-11}$	$3{\cdot}5031 \times 10^{-8}$	$3{\cdot}3490 \times 10^{-8}$
A_{11}	$8{\cdot}4078 \times 10^{-19}$	$2{\cdot}9449 \times 10^{-21}$	$8{\cdot}2670 \times 10^{-14}$	$1{\cdot}0375 \times 10^{-14}$	$3{\cdot}2665 \times 10^{-10}$	$2{\cdot}0987 \times 10^{-10}$
A_{13}	$1{\cdot}2303 \times 10^{-21}$	$1{\cdot}2240 \times 10^{-21}$	$8{\cdot}5657 \times 10^{-16}$	$8{\cdot}8824 \times 10^{-16}$	$9{\cdot}1147 \times 10^{-12}$	$1{\cdot}0364 \times 10^{-11}$
A_{15}	$2{\cdot}0814 \times 10^{-25}$	$6{\cdot}1959 \times 10^{-25}$	$1{\cdot}3162 \times 10^{-18}$	$3{\cdot}3308 \times 10^{-18}$	$1{\cdot}0784 \times 10^{-13}$	$1{\cdot}3677 \times 10^{-13}$
A_{17}	$3{\cdot}1505 \times 10^{-28}$	$2{\cdot}4451 \times 10^{-31}$	$1{\cdot}3261 \times 10^{-20}$	$3{\cdot}5987 \times 10^{-22}$	$2{\cdot}5875 \times 10^{-15}$	$6{\cdot}7674 \times 10^{-16}$

Table 4. Distribution of hydrodynamic potential, ϕ_s/D, on the surface of a rod located in the interior of a rod bundle

β, degrees	$D/P = 0{\cdot}30$ Bank 1	$D/P = 0{\cdot}30$ Bank 2	$D/P = 0{\cdot}50$ Bank 1	$D/P = 0{\cdot}50$ Bank 2	$D/P = 0{\cdot}70$ Bank 1	$D/P = 0{\cdot}70$ Bank 2
0	1·080	1·076	1·253	1·239	1·648	1·601
30	0·936	0·932	1·094	1·080	1·467	1·423
60	0·542	0·539	0·645	0·631	0·913	0·878
90	0·0008	−0·002	0·004	−0·008	0·009	−0·020
120	−0·541	−0·541	−0·638	−0·643	−0·884	−0·918
150	−0·937	−0·931	−1·098	−1·070	−1·473	−1·409
180	−1·082	−1·072	−1·265	−1·215	−1·692	−1·506

Theoretical justification of this assumption is possible using the mathematical expression of potential distribution on the cylindrical surface given by (25). The results of the calculation, carried out with the aid of an IBM 7094 computer, are shown in Table 4 for three different D/P ratios. Comparisons of these calculated values of Φ_s with the cosine curves represented by (36), are shown in Figs. 9 and 10. For low values of D/P, as can be observed, the distribution of the surface potential, Φ_s, is well represented by (36). It can also be noted that the distribution is approximately symmetrical with respect to the angle $\beta = \pi/2$. At the limit where D/P approaches zero, the distribution will become completely symmetrical, as indicated by (25). This corresponds to the case where a single cylinder is placed in a uniform-velocity stream. For larger values of D/P, slight deviation from (36) occurs. Generally speaking, however, (36) is a good approximation for the distribution of the surface potential.

(b) *Nusselt number, Nu_D, for cosine surface temperature distribution.* If the Nusselt number is based upon a mean value of the local heat-transfer coefficient, then, from (37) and (40),

$$h(\phi) = \frac{q''(\phi)}{T(\phi)} = 2\sqrt{[(kC_v V\rho)/(\pi\phi)]}.$$

Therefore, the average heat-transfer coefficient in the $[\psi, \phi]$ domain can be written as

$$\bar{h} = \frac{2}{\phi_1}\sqrt{[(kC_v\rho V)/(\pi\phi)]}\int_0^{\phi_1}\phi^{-1/2}\,d\phi =$$

$$= 4\sqrt{[(kC_v\rho V)/(\pi\phi_1)]}. \quad (47)$$

To convert this to the r, θ domain, it is noted that $\bar{h}\phi_1 = h_D(\pi D/2)$.

Hence,

$$h_D = \bar{h}(2\phi_1/\pi D) = \frac{8}{\pi D}\sqrt{[(kC_v\rho V\phi_1)/\pi]}$$

and the expression for the Nusselt number, Nu_D, becomes

$$Nu_D = \frac{h_D D}{k} = \frac{8}{\pi^{3/2}} \sqrt{[(\rho C_v V D)/k]}\,(\phi_1/D)^{1/2}$$

or

$$Nu_D = 1{\cdot}437\,(\phi_1/D)^{1/2}\,(Pe)^{1/2}. \tag{48}$$

Comparison of (48) with (44) shows that, for the cosine surface temperature distribution defined by (35), the numerical values of the two types of Nusselt numbers can differ by as much as 50 per cent. It should be point out, however, that Nu_D has much less practical significance than does Nu_t.

(c) *Nusselt number, Nu_t, for constant surface heat flux.* In the analysis given by Grosh and Cess [4, 5], the Nusselt number, Nu_t, corresponding to a constant heat flux from the surface of a cylinder, was not obtained. Since all experimental results have been nominally obtained for constant heat flux conditions, the Nusselt number for this case will be derived. This derivation is based on a cylinder located in the interior of a rod bundle, with the assumption of the hydrodynamic potential distribution given by (36).

Inasmuch as heat flux is on an area basis, the expression for heat flux as a function of ϕ can be written

$$q''(\phi) = q''\,\frac{ds}{d\phi}$$

where q'' is the constant surface heat flux in the r, θ domain. From (36), and also from the relationship giving the length of arc along the surface of a cylinder, $s = D\beta/2$, $ds/d\phi$ can be expressed as

$$\frac{ds}{d\phi} = \frac{D}{\phi_1 \sin\beta} = \frac{D}{2\sqrt{[\phi\,(\phi_1 - \phi)]}}.$$

Therefore,

$$q''(\phi) = \frac{q'' D}{2\sqrt{[\phi\,(\phi_1 - \phi)]}}. \tag{49}$$

The solution of (34) for the case in which the surface heat flux is $q''(\phi)$ is given as [3],

$$T'(\phi) = \frac{1}{k}\sqrt{[\kappa/(\pi V)]}\int_0^\phi q''(\phi - \delta)\,(d\delta/\sqrt{\delta}). \tag{50}$$

Thus,

$$T'(\phi) = \frac{q'' D}{2k}(\kappa/\pi V)^{1/2}\int_0^\phi \frac{d\delta}{\sqrt{[\delta(\phi - \delta)\,(\phi_1 - \phi + \delta)]}} = \frac{q'' D}{k\sqrt{\phi_1}}(\kappa/\pi V)^{1/2}\int_0^{\pi/2}\frac{d\omega}{[1 - (\phi/\phi_1)\sin^2\omega]^{1/2}}. \tag{51}$$

In the above equation, the integral is a complete elliptic integral of the first kind. Since

$$\phi/\phi_1 = (1 - \cos\beta)/2$$

the local surface temperature in the r, θ domain can be written as

$$T'(\beta) = \frac{q'' D}{k}(\kappa/\pi V \phi_1)^{1/2}\int_0^{\pi/2}\frac{d\omega}{[1 - \{(1 - \cos\beta)/2\}\sin^2\omega]^{1/2}}. \tag{52}$$

The average temperature over the surface of the cylinder is therefore,

$$\bar{T}' = \frac{q'' D}{\pi k}(\kappa/\pi V \phi_1)^{1/2}\int_0^\pi\int_0^{\pi/2}\frac{d\omega\,d\beta}{[1 - \{(1 - \cos\beta)/2\}\sin^2\omega]^{1/2}}. \tag{53}$$

The heat-transfer coefficient, h_t, based upon the average surface temperature is then

$$h_t = \frac{[(\pi k\sqrt{\phi_1})/D]\,[(\pi\rho C_v V)/k]^{1/2}}{\displaystyle\int_0^\pi\int_0^{\pi/2}\frac{d\omega\,d\beta}{[1 - \{(1 - \cos\beta)/2\}\sin^2\omega]^{1/2}}} \tag{54}$$

and hence, the Nusselt number, Nu_t, becomes

$$Nu_t = \frac{h_t D}{k} = \frac{\pi^{3/2}\,[(\rho C_v V D)/k]^{1/2}\,(\phi_1/D)^{1/2}}{\int_0^\pi K[\sin(\beta/2)]\,d\beta} \tag{55}$$

where $K\,[\sin(\beta/2)]$ denotes the elliptic integral; this equation can be reduced to

$$Nu_t = \frac{5{\cdot}5683\,\sqrt{(Pe)}\,\sqrt{(\phi_1/D)}}{\int_0^\pi K[\sin(\beta/2)]\,d\beta}. \tag{56}$$

The integral in the denominator of this equation was evaluated graphically. The final

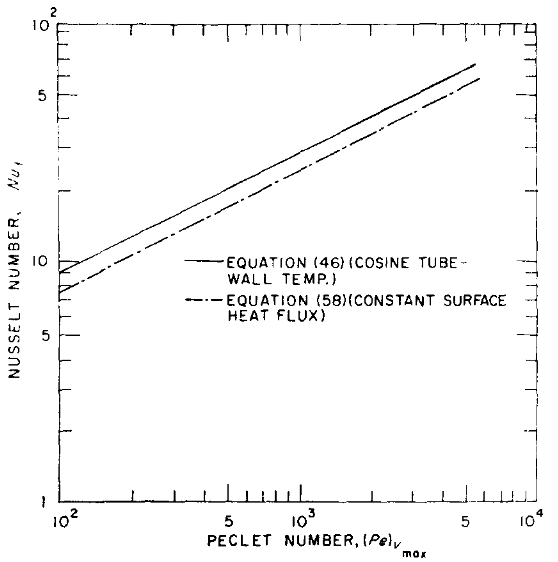

FIG. 11. Comparison of theoretical Nusselt numbers obtained by assuming (a) cosine tube-wall temperature distribution, (b) constant surface heat flux from tube wall.

expression becomes

$$Nu_t = 0{\cdot}81\ (\phi_1/D)^{1/2}\,(Pe)^{1/2} \tag{57}$$

or, alternatively, it can be written,

$$Nu_t = 0{\cdot}81\ (\phi_1/D)^{1/2}\,(Pe)^{1/2}_{V_{\max}}\,(V/V_{\max})^{1/2}. \tag{58}$$

For the case in which a single rod is placed in the fluid stream, a similar derivation can be followed. For this case, the Nusselt number was obtained as follows:

$$Nu_t = \frac{7{\cdot}8736\,(Pe)^{1/2}}{\int_0^{\pi} K\,[\sin(\beta/2)]\,\mathrm{d}\beta} = 1{\cdot}145\,(Pe)^{1/2}. \tag{59}$$

In Fig. 11, (58) is compared with (46). As can be seen, the theoretical predictions for the Nusselt number, using (58), fall somewhat lower than that calculated from (46). It is therefore, apparent that in the experimental investigations cited, circumferential heat conduction in the cylinder cannot be completely ignored.

CONCLUSIONS

The results of the present investigation are summarized as follows:

(1) For potential flow across rod bundles, or tube banks, the theoretical expression for the hydrodynamic potential drop, ϕ_1/D, for a cylinder located in the interior of a rod bundle is obtained by utilizing a special mathematical function originally proposed by Howland and McMullen. Computation of numerical values of ϕ_1/D is made for two typical tube-bank geometries. The results are presented in tabular form.

(2) By assuming that the circumferential variation of both the tube-wall temperature and the hydrodynamic potential can be represented by a cosine-type distribution, an expression for Nusselt's number, Nu_t, is obtained by applying inviscid flow theory. This expression predicts Nusselt numbers which agree well with the experimental results.

(3) For a rod located in the interior of the rod bundle, the distribution of hydrodynamic potential around the cylindrical surface can be satisfactorily approximated by a cosine-type distribution.

ACKNOWLEDGEMENTS

The author wishes to express his appreciation to Dr. O. E. Dwyer for his suggesting the problem and giving kind advice during the course of the study. Discussions with Professor W. T. Snyder of the State University of New York at Stony Brook, were also most valuable.

REFERENCES

1. V. M. BORISHANSKII, A. A. ANDREEVSKII and V. B. ZHINKINA, Heat transfer to cross-flowing liquid sodium in a staggered tube bank, *Atomnaya Energiya (USSR)* **13**, 9, 269–271 (1962).
2. M. J. BOUSSINESQ, Calcul du pouvoir refroidissant des courants fluids, *J. Math.* **1**, 285 (1905).
3. H. S. CARSLAW and J. C. JEAGER, *Conduction of Heat in Solids*. Oxford University Press, London (1958).
4. R. J. GROSH and R. D. CESS, Heat transfer to fluids with low Prandtl numbers for flow across plates and cylinders of various cross section, *Trans. ASME* **80**, 667 (1958).
5. R. D. CESS and R. J. GROSH, Heat transmission to fluids with low Prandtl numbers for flow through tube banks, *Trans. ASME* **80**, 677 (1958).
6. R. J. HOE, D. DROPKIN and O. E. DWYER, Heat transfer rates to cross flowing mercury in a staggered tube bank—I, *Trans. ASME* **79**, 899 (1957).
7. R. C. J. HOWLAND and B. W. MCMULLEN, Potential functions related to groups of circular cylinders, *Cambridge Phil. Soc.* **32**, 402 (1936).
8. M. W. MARESCA and O. E. DWYER, Heat transfer to mercury flowing in-line through a bundle of circular rods. Accepted for publication in *ASME J. Heat Transfer*.
9. C. L. RICKARD, O. E. DWYER and D. DROPKIN, Heat transfer rates to cross-flowing mercury in a staggered tube bank—II, *Trans. ASME* **80**, 646 (1958).

Résumé—On a obtenu des expressions théoriques améliorées pour les nombres de Nusselt dans l écoulement transversal de métaux liquides à travers des faisceaux de barres, en appliquant l'analyse en fluide non-visqueux [4, 5]. Les développements théoriques sont basés sur l'hypothèse que, pour une barre placée à l'intérieur d'un faisceau, les variations circonférentielles de la température de la paroi du tube et du potentiel hydrodynamique peuvent être exprimées par des distributions en cosinus. La première hypothèse est déduite des observations expérimentales de Hoe *et al.* [6], avec des conditions dans lesquelles le flux de chaleur était apparemment presque uniforme, et la dernière hypothèse est postulée sur la base de considérations théoriques. Avec ces hypothèses, l'expression suivante pour le nombre de Nusselt, semblable à celle de Cess et Grosh [5], devient:

$$Nu_t = 0{,}958\,(\phi_1/D)^{\frac{1}{2}}\,(Pe)^{\frac{1}{2}}{}_{V_{\max}}\,(V/V_{max})^{\frac{1}{2}}.$$

L'expression ci-dessus prédit des nombres de Nusselt qui sont en bon accord avec les résultats expérimentaux obtenus précédemment au Laboratoire National de Brookhaven [6, 9]. On a aussi présenté une méthode théorique de détermination des valeurs du paramètre, ϕ_1/D, chute de potentiel hydrodynamique normalisée. Les résultats sont en bon accord avec ceux obtenus expérimentalement par Cess et Grosh [5]. On a obtenu une expression analytique pour ϕ_1/D en utilisant ces fonctions mathématiques développées originellement par Howland et McMullen [7]. Les valeurs théoriques de ϕ_1/D pour l'écoulement à travers deux géométries typiques de faisceaux de tubes, c'est à dire l'espacement en carrés et l'espacement en triangles équilatéraux, ont été obtenues à l'aide d'un calculateur numérique à grande vitesse. On a présenté les résultats numériques sous forme de tableaux.

Zusammenfussung—Durch Anwendung der Analysis reibungsfreier Strömungen [4, 5] erhält man verbesserte theoretische Ausdrücke für Nusseltzahlen bei flüssigen Metallen in quer angeströmten Rohrbündeln. Die theoretischen Ableitungen beruhen auf der Annahme, dass für einen Stab im Innern des Bündels die Umfangsänderung der Wandtemperatur und des hydrodynamischen Potentials durch eine kosinusartige Verteilung wiedergegeben werden kann. Die erstere Annahme ist aus den experimentellen Beobachtungen von Hoe und anderen [6] abgeleitet. Der Wärmefluss war dabei nahezu gleichförmig. Die letztere Annahme erscheint auf Grund theoretischer Beobachtungen gerechtfertigt. Mit diesen Annahmen ergibt sich, ähnlich wie bei Cess und Grosh [5] folgender Ausdruck für die Nusseltzahl:

$$Nu_t = 0{,}958\,(\phi_1/D)^{\frac{1}{2}}\,(Pe)^{\frac{1}{2}}{}_{V_{\max}}\,(V/V_{\max})^{\frac{1}{2}}.$$

Die nach obiger Gleichung errechneten Nusseltzahlen stimmen gut mit kürzlich in Brookhaven National Laboratory [6, 9] erhaltenen experimentellen Ergebnissen überein. Eine theoretische Methode doe Werte des Parameters ϕ_1/D des hydrodynamischen Potentialgefälles zu bestimmen, ist ebenfalls angegeben. Die Ergebnisse stimmen gut mit den von Cess und Grosh [5] experimentell erhaltenen überein. Ein analytischer Ausdruck für ϕ_1/D lässt sich mit Hilfe ursprünglich von Howland und McMullen entwickelter mathematischer Funktionen [7] angeben. Die theoretischen Werte von ϕ_1/D für die Anströmung zweier typischer Anordnungen der Rohre im Rohrbündel nämlich in der Form von Quadraten und von gleichseitigen Dreiecken wurden mit Hilfe eines Hochgeschwindigkeitsdigitalrechners erhalten. Die numerischen Ergebnisse sind in Tabellenform wiedergegeben.

Аннотация—На основе анализа невязкого течения [4, 5] получены новые теоретические выражения чисел Нуссельта при поперечном течении жидких металлов через пучки стержней. Теоретические выводы основаны на допущении, что для стержня, расположенного внутри пучка, изменение по периметру температуры стенки трубы и гидродинамического потенциала выражается косинусоидальным распределением. Это наблюдение выведено из экспериментальных наблюдений Хоу и др. [6] в условиях, когда тепловой поток был явно близок к однородному; последнее постулируется на основе теоретического анализа. При таких допущениях получаем следующее выражение для числа Нуссельта, подобное полученному Цессом и Грошем [5]:

$$Nu_t = 0{,}958\,(\phi_1/D)^{\frac{1}{2}}\,(Pe)^{\frac{1}{2}}{}_{V_{\max}}\,(V/V_{\max})^{\frac{1}{2}}.$$

Это выражение дает значения чисел Нуссельта, которые хорошо согласуются с экспериментальными результатами, полученными ранее в Национальной лаборатории Брукхевена [6, 9].

Также представлен теоретический метод определения значений параметра ϕ_1/D и перепада гидродинамического потенциала. Результаты хорошо согласуются с экспериментальными данными Цесса и Гроша [5]. Используя математические функции, первоначально выведенные Хаулендом и Мак-Мюлленом [7], найдено аналитическое выражение для ϕ_1/D. С помощью быстродействующей цифровой вычислительной машины получены теоретические значения ϕ_1/D для течения через два обычного вида пучка труб: по квадратам и равнобедренным треугольникам. Численные результаты представлены в виде таблиц.